

Activation of the cGMP/PKG pathway inhibits electrical activity in rabbit urethral interstitial cells of Cajal by reducing the spatial spread of Ca^{2+} waves

G. P. Sergeant, Louise Johnston, N. G. McHale, K. D. Thornbury and M. A. Hollywood

Smooth Muscle Research Centre, Dundalk Institute of Technology, Dublin Road, Dundalk, Co. Louth, Ireland

In the present study we used a combination of patch clamping and fast confocal Ca^{2+} imaging to examine the effects of activators of the nitric oxide (NO)/cGMP pathway on pacemaker activity in freshly dispersed ICC from the rabbit urethra, using the amphotericin B perforated patch configuration of the patch-clamp technique. The nitric oxide donor, DEA-NO, the soluble guanylyl cyclase activator YC-1 and the membrane-permeant analogue of cGMP, 8-Br-cGMP inhibited spontaneous transient depolarizations (STDs) and spontaneous transient inward currents (STICs) recorded under current-clamp and voltage-clamp conditions, respectively. Caffeine-evoked Cl^- currents were unaltered in the presence of SP-8-Br-PET-cGMPs, suggesting that activation of the cGMP/PKG pathway does not block Cl^- channels directly or interfere with Ca^{2+} release via ryanodine receptors (RyR). However, noradrenaline-evoked Cl^- currents were attenuated by SP-8-Br-PET-cGMPs, suggesting that activation of cGMP-dependent protein kinase (PKG) may modulate release of Ca^{2+} via IP_3 receptors (IP_3R). When urethral interstitial cells (ICC) were loaded with Fluo4-AM ($2\ \mu\text{M}$), and viewed with a confocal microscope, they fired regular propagating Ca^{2+} waves, which originated in one or more regions of the cell. Application of DEA-NO or other activators of the cGMP/PKG pathway did not significantly affect the oscillation frequency of these cells, but did significantly reduce their spatial spread. These effects were mimicked by the IP_3R blocker, 2-APB ($100\ \mu\text{M}$). These data suggest that NO donors and activators of the cGMP pathway inhibit electrical activity of urethral ICC by reducing the spatial spread of Ca^{2+} waves, rather than decreasing wave frequency.

(Received 1 March 2006; accepted after revision 14 April 2006; first published online 27 April 2006)

Corresponding author M. A. Hollywood: Smooth Muscle Research Centre, Dundalk Institute of Technology, Dublin Road, Dundalk, Co. Louth, Ireland. Email: mark.hollywood@dkit.ie

Nitric oxide (NO) is the main inhibitory neurotransmitter in the urethra of a variety of species including rabbits, rats, sheep, pigs and humans (for review see Andersson & Wein, 2000). A number of studies have demonstrated that either electrical field stimulation of inhibitory nerves or exogenous application of NO can elevate cGMP levels in this tissue (Morita *et al.* 1992; Dokita *et al.* 1994; Persson & Andersson, 1994). Furthermore, mice lacking cGMP-dependent protein kinase G_1 (PKG_1 , Persson *et al.* 2000) have significantly attenuated neurogenic relaxation of the urethra, suggesting that PKG_1 is essential for nitric-mediated relaxation.

Although it is now well established that NO mediates its effects on the urethra via the cGMP/ PKG_1 pathway, little is known about how this inhibits urethral tone. One possibility is that NO reduces urethral tone by inhibiting the underlying spontaneous electrical activity. The effects

of NO and NO donors on urethral electrical activity have been briefly examined in the rabbit urethra, but the results have been equivocal. Ito & Kimoto (1985) demonstrated that inhibitory junction potentials could be elicited by transmural nerve stimulation in the rabbit urethra and suggested that these were mediated via a non adrenergic non cholinergic (NANC) neurotransmitter. Although Hashitani *et al.* (1996) demonstrated that sodium nitroprusside application reduced the frequency of slow waves in the same tissue, they failed to demonstrate any hyperpolarization associated with this effect. Waldeck *et al.* (1998) were unable to demonstrate any effect of exogenous NO or inhibitory nerve stimulation on electrical activity in the same tissue. The results from the latter studies (Waldeck *et al.* 1998; Hashitani *et al.* 1996) combined with the insensitivity of the relaxant response to K^+ channel blockers (Garcia-Pascual & Triguero, 1994;

Costa, Labadia, Triguero, Jimenez & Garcia-Pascual, 2001) suggest that in contrast to other smooth muscles, K^+ channels contribute little to NO-mediated relaxation in the urethra.

More recent studies have demonstrated that urethral tone may be generated (Sergeant *et al.* 2000) and modulated (Sergeant *et al.* 2002; Smet *et al.* 1996; Waldeck *et al.* 1998) by specialized pacemaker cells. These cells generate spontaneous transient inward Cl^- currents in the rabbit urethra, which are thought to drive the surrounding smooth muscle in a manner similar to that demonstrated for interstitial cells of Cajal (ICC) in the gastrointestinal tract (Sanders, Koh & Ward, 2005). We have previously suggested that noradrenergic neurotransmission may, in part at least, be mediated via activation of urethral ICC. Immunohistochemical evidence presented by Smet *et al.* (1996) and Waldeck *et al.* (1998) would also support our contention that urethral ICC play a role in neurotransmission. Their studies demonstrated the presence of branched interstitial cells in the human, guinea-pig and rabbit urethras, respectively, that were immunopositive for cGMP, and support the idea that they may be important in mediating neurally released NO responses.

However, no study has examined in detail the effects of activating the cGMP/PKG pathway on electrical activity in isolated ICC from the rabbit urethra. The purpose of the present study was to examine the effects of activating the cGMP/PKG on electrical activity and Ca^{2+} waves, using a combination of electrophysiology and confocal imaging on freshly dispersed ICC from the rabbit urethra.

Methods

Cell dispersal

The bladder and urethra were removed from both male and female rabbits immediately after they had been killed by lethal injection of pentobarbitone. The most proximal 3 cm of the urethra was removed and placed in Krebs solution. This was then opened up longitudinally and the urothelium removed by sharp dissection. Strips of tissue, 0.5 cm in width were cut into 1 mm^3 pieces and stored in Hanks Ca^{2+} free solution for 30 min at 4°C prior to cell dispersal. Tissue pieces were incubated in dispersal medium containing (per 5 ml of Ca^{2+} -free Hanks solution (see Solutions)): 15 mg collagenase (Sigma type 1A), 1 mg protease (Sigma type XXIV), 10 mg bovine serum albumin (Sigma) and 10 mg trypsin inhibitor (Sigma) for 10–15 min at 37°C . Tissue was then transferred to Ca^{2+} -free Hanks solution, and stirred for a further 15–30 min to release single smooth muscle cells and ICC. These cells were plated in Petri dishes containing $100\ \mu\text{M}$ Ca^{2+} Hanks solution and stored at 4°C for use within 8 h.

Using our dispersal procedure, both ICC and smooth muscle cells could be reliably isolated from the rabbit

urethra as previously described (Sergeant *et al.* 2000). In the present study we focused on studying interstitial cells, which could be easily distinguished from smooth muscle cells using a number of criteria (Sergeant *et al.* 2000). Thus, ICC were highly branched, failed to contract in response to depolarizing current injection or application of noradrenaline, possessed abundant calcium-activated chloride current and normally fired spontaneous transient inward currents under voltage-clamp conditions.

Perforated-patch recordings from single cells

Currents were recorded using the perforated-patch configuration of the whole-cell patch-clamp technique (Rae *et al.* 1991). This circumvented the problem of current rundown encountered using the conventional whole-cell configuration. The cell membrane was perforated using the antibiotic amphotericin B ($600\ \mu\text{g ml}^{-1}$). Patch pipettes were initially front-filled by dipping into pipette solution, and then back-filled with the amphotericin B-containing solution. Pipettes were pulled from borosilicate glass capillary tubing (1.5 mm outer diameter, 1.17 mm inner diameter; Clark Medical Instruments) to a tip of diameter approximately 1–1.5 μm and resistance of 2–4 $\text{M}\Omega$.

Voltage-clamp commands were delivered via an Axopatch 1D patch clamp amplifier (Axon Instruments) and membrane currents were recorded by a 12-bit AD/DA converter (Axodata 1200 or Labmaster, Scientific Solutions) interfaced to an Intel computer running pClamp software. During experiments, the dish containing the cells was continuously perfused with Hanks solution at $36 \pm 1^\circ\text{C}$. Additionally the cell under study was continuously superfused by means of a custom-built close delivery system with a pipette of tip diameter 200 μm placed approximately 300 μm from the cell. The Hanks solution in the close delivery system could be switched to a drug-containing solution with a dead space time of less than 5 s. In all experiments, *n* refers to the number of cells studied, and each experimental set usually contained samples from a minimum of four animals. Summary data are presented as the mean \pm standard error (s.e.m.), and statistical comparisons were made on raw data using Students' paired *t* test, taking $P < 0.05$ level as significant. In all figures *represents $P < 0.05$ and ** represents $P < 0.01$. The frequency of spontaneous transient inward currents (STICs) was obtained by measuring events that had amplitudes greater or equal to 100 pA and durations greater or equal to 500 ms. Similarly, any spontaneous transient depolarisation (STD) that had a duration of less than 500 ms was excluded from the analysis.

Ca^{2+} imaging of single ICCs

After isolation of single cells, these were plated onto glass-bottomed dishes (WillCo) and left to stick down for

30 min on the microscope stage. They were then incubated in the dark for 15 min at room temperature with an acetoxymethylester form of the Ca^{2+} -sensitive fluorescent dye Fluo4-AM ($2 \mu\text{M}$) and washed with warmed normal Hanks solution for 30 min prior to experimentation.

Cells were maintained at 37°C in normal Hanks solution and imaged using either an iXon 887 EMCCD camera (Andor Technology, Belfast; 512×512 pixels, pixel size $16 \times 16 \mu\text{M}$) coupled to a Nipkow spinning disk confocal head (CSU22, Yokogawa, Japan) or a MegaXR10 GenIII+ ICCD (Stanford Photonics, USA; 1024×1000 pixels, pixel size $7 \times 7 \mu\text{M}$) attached to a Nipkow spinning disk confocal head (CSU10, Visitech UK). A krypton-argon laser (Melles Griot UK) at 488 nm was used to excite the Fluo-4, and the emitted light was detected at wavelengths >510 nm. Images were usually acquired at 5 or 15 frames s^{-1} and analysed using custom-written macros for Image J. These macros were kindly written by Dr Tony Collins, Wright Cell Imaging Facility, University Health Network, Toronto, Canada.

Image analysis

To analyse the data from confocal microscopy experiments, the mean camera background was first subtracted. Images were then normalized to obtain F/F_0 by dividing the entire image by the mean intensity of the cell during a quiescent phase (i.e. the minimum fluorescence obtained between waves). Whole cell wave intensity was determined by drawing a region of interest (ROI) around the cell and plotting out the mean intensity.

To obtain *post hoc* linescan images, a 1 pixel-thick line was drawn centrally through the entire length of the cell and the 'reslice' command in Image J was invoked.

To measure wave propagation, the F/F_0 images were thresholded to 75% of the peak wave intensity, and the distance at which the wave remained above threshold was taken as the propagation distance.

Solutions

The composition of the solutions used was as follows (mM): (1) Hanks solution: 129.8 Na^+ , 5.8 K^+ , 135 Cl^- , 4.17 HCO_3^- , 0.34 HPO_4^{2-} , $0.44 \text{ H}_2\text{PO}_4^-$, 1.8 Ca^{2+} , 0.9 Mg^{2+} , 0.4 SO_4^{2-} , 10 glucose, 2.9 sucrose and 10 Hepes, pH adjusted to 7.4 with NaOH. (2) Cs^+ perforated patch pipette solution: 133 Cs^+ , 135 Cl^- , 1.0 Mg^{2+} , 0.5 EGTA , 10 Hepes, pH adjusted to 7.2 with CsOH. (3) Krebs solution: 146.2 Na^+ , 5.9 K^+ , 133.3 Cl^- , 25 HCO_3^- , $1.2 \text{ H}_2\text{PO}_4^-$, 2.5 Ca^{2+} , 1.2 Mg^{2+} and 11 glucose, pH maintained at 7.4 by bubbling with 95% O_2 , 5% CO_2 . (4) Ca^{2+} -free Hanks solution: 129.8 Na^+ , 5.8 K^+ , 135 Cl^- , 4.17 HCO_3^- , 0.34 HPO_4^{2-} , $0.44 \text{ H}_2\text{PO}_4^-$, 2.7 Mg^{2+} , 0.4 SO_4^{2-} , 10 glucose, 2.9 sucrose, 5 EGTA and 10 Hepes, pH adjusted to 7.4 with NaOH.

Drugs used

The following drugs were used: amphotericin B (Sigma), 3-(5-hydroxymethyl-2-furyl)-1-benzyl indazole (YC-1, 100 mM stock in H_2O) diethylamine nitric oxide (DEA-NO, Tocris; 100 mM stock in 10 mM NaOH), 8-Br-cGMP (Tocris, 100 mM stock in H_2O), β -Phenyl-1, N^2 -etheno-8-bromoguanosine-3', 5'-cyclic monophosphorothioate- (SP-8-Br-PET-cGMPs, Biolog, 10 mM stock in H_2O), noradrenaline (Levophed, Zanofti Winthrop, added directly to Hanks), caffeine (Sigma, added directly to Hanks), 2-aminoethoxy diphenyl-borate (2-APB, Acros, 100 mM stock in 50% ethanol), 2-nitro-4-carboxyphenyl- N,N -diphenylcarbamate (NCDC, Sigma, 100 mM stock in DMSO). All drugs were diluted to their final concentrations in Hanks solution. Drug vehicles had no effect on the currents or Ca^{2+} oscillations studied.

Results

Effect of DEA-NO on spontaneous electrical activity of isolated ICC

When isolated ICCs were held under current clamp with Cs^+ -rich pipettes, a small background hyperpolarizing current had to be injected to bring membrane potential to ~ -60 mV. In the absence of any drugs, the ICC in Fig. 1A, fired STDs at a frequency of 12 min^{-1} . Upon application of DEA-NO ($30 \mu\text{M}$), the frequency of STDs was reduced to $\sim 2 \text{ min}^{-1}$, and returned towards control upon washout. Figure 1B shows a summary of four similar experiments in which the frequency of STDs was measured before, during and after washout of DEA-NO. Application of the NO donor significantly reduced STD frequency from $6.8 \pm 1.9 \text{ min}^{-1}$ to $0.8 \pm 0.5 \text{ min}^{-1}$ ($P < 0.05$).

To test the effects of NO on spontaneous transient inward currents (STICs), which, it has been previously shown, underlie STDs (Sergeant *et al.* 2000), we examined the effects of DEA-NO on STICs in ICC held at -60 mV under voltage-clamp conditions. As Fig. 1C suggests DEA-NO ($30 \mu\text{M}$) rapidly and reversibly abolished the STICs. In nine similar experiments (Fig. 3D), DEA-NO significantly reduced the frequency of STICs from 7 ± 1.8 to $1 \pm 0.6 \text{ min}^{-1}$ ($P < 0.01$). Upon washout, the frequency of STICs returned $5.6 \pm 2.3 \text{ min}^{-1}$, which was not significantly different from the control.

Effect of activating cGMP on spontaneous electrical activity in isolated ICC

Since NO is thought to mediate its effects via the cGMP/PKG pathway, we next assessed if the effects of DEA-NO could be mimicked by the membrane-permeant activator of soluble guanylyl cyclase, YC-1 and the membrane permeant-analogue of cGMP, 8-Br-cGMP. As

Fig. 2A–D suggests, activation of guanylyl cyclase with YC-1 ($30 \mu\text{M}$) decreased the frequency of STDs and STICs in ICCs in a manner similar to that observed with DEA-NO. Figure 2B and D shows summary data from a series of experiments in which the frequency of STDs and STICs, respectively, was measured before, during and after application of YC-1. The frequency of STDs was reduced from $9.0 \pm 2.1 \text{ min}^{-1}$ to $0.8 \pm 0.5 \text{ min}^{-1}$ ($n = 5, P < 0.01$). Similarly, STIC frequency was reversibly reduced in six experiments, from $12.8 \pm 1.2 \text{ min}^{-1}$ to $5.3 \pm 1.4 \text{ min}^{-1}$ in the presence of YC-1 ($P < 0.01$).

When the effects of 8-Br-cGMP (1 mM) were examined (Fig. 2E–H), the frequency and amplitude of both STDs (Fig. 2E) and STICs (Fig. 2G) were reversibly reduced. Figure 2F and H shows summaries of four experiments in which 8-Br-cGMP decreased STD and STIC frequency from 11.6 ± 3.4 to 0.9 ± 1 ($P < 0.01$) and from $11 \pm 3 \text{ min}^{-1}$ to $1.5 \pm 0.9 \text{ min}^{-1}$, respectively ($P < 0.05$).

Effect of activating the GC/cGMP pathway on spontaneous Ca^{2+} events

In an attempt to understand how activating the cGMP/PKG-dependent pathway could alter the Ca^{2+} events underlying STICs in ICCs, we carried out a series of experiments on freshly dispersed ICCs loaded with the Ca^{2+} indicator Fluo4-AM. Under control conditions the Ca^{2+} events were quite variable from cell to cell as noted previously (Johnston *et al.* 2005). In approximately 50% of the cells studied, spontaneous Ca^{2+} waves were observed. These occurred at a mean frequency of $4.1 \pm 0.5 \text{ min}^{-1}$, had a mean amplitude of $4.4 \pm 0.4 F/F_0$, full duration at half maximum amplitude (FDHM) of $2.9 \pm 0.4 \text{ s}$, a mean spatial spread of $112 \pm 12 \mu\text{m}$, and a mean propagation speed of $27 \pm 0.4 \mu\text{m s}^{-1}$ ($n = 14$). Since these events underlie the generation of STICs in urethral ICCs (Johnston *et al.* 2005), we focused on studying these waves in the present study.

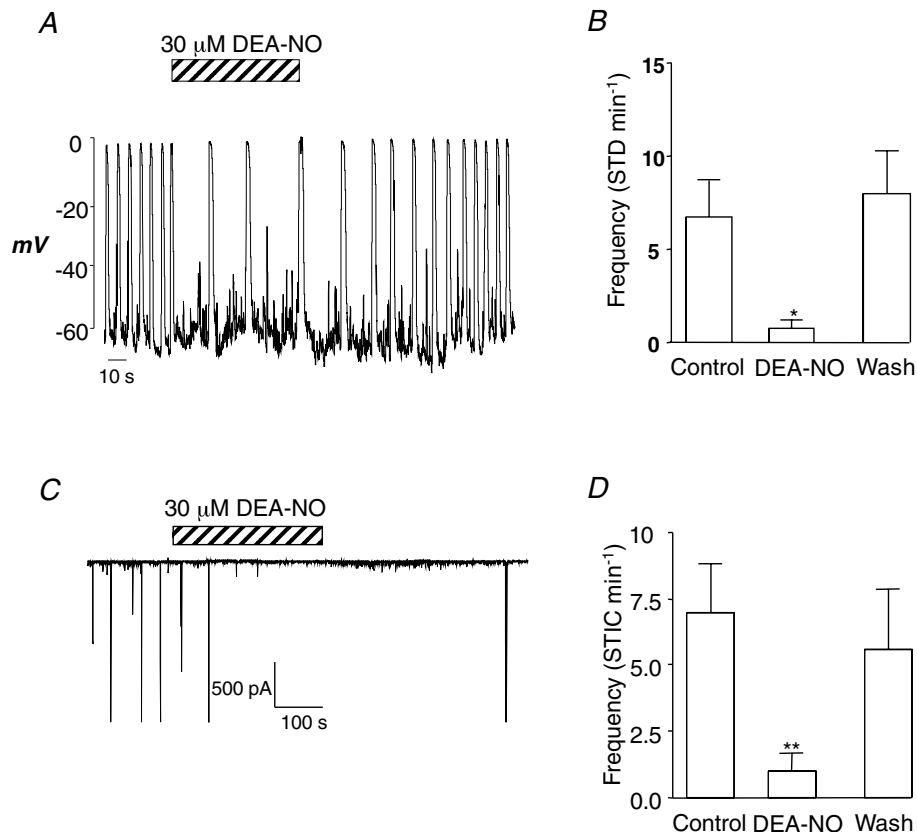


Figure 1. DEA-NO reversibly inhibits slow waves and STICs in urethral ICC

A, the effect of DEA-NO ($30 \mu\text{M}$) on a spontaneously active single ICC under current-clamp conditions. B, summary data of the effects of DEA-NO on STD frequency in four experiments recorded under the same conditions as A. C, a typical effect of DEA-NO on STICs recorded from an ICC held under voltage clamp at -60 mV . D, a summary of the effect of DEA-NO on STIC frequency, obtained from six experiments recorded under the same conditions as C.

Effect of DEA-NO on spontaneous Ca²⁺ events

Figure 3 shows a typical example of an experiment in which the effect of DEA-NO was examined on a spontaneously active ICC recorded at 5 frames per second (fps). Figure 3A

shows a plot of whole-cell fluorescence against time, and demonstrates that application of DEA-NO (30 μM) reduced the amplitude of the Ca²⁺ waves but had little effect on their frequency. In 17 similar experiments

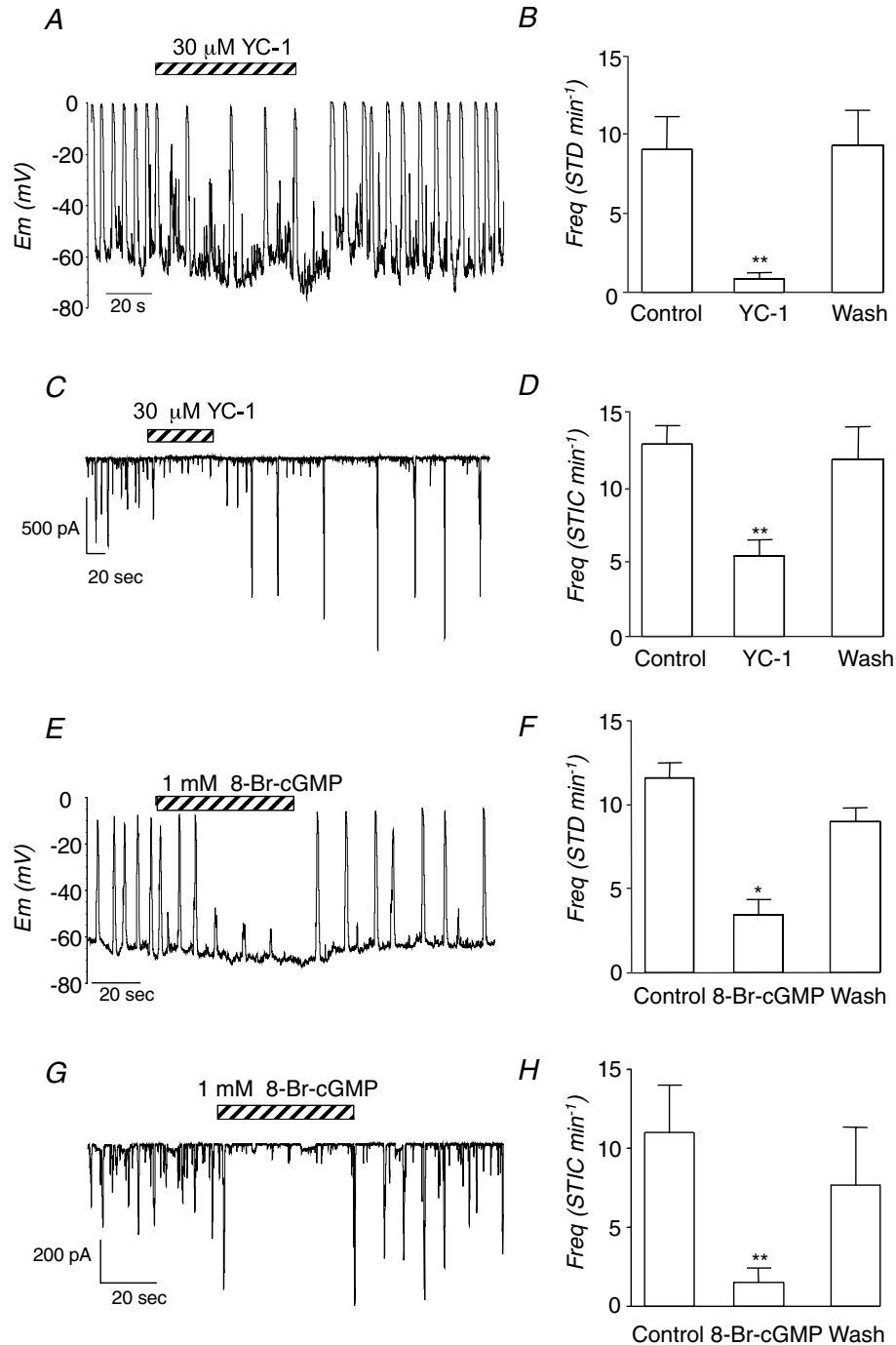


Figure 2. Activators of the cGMP/GK pathway inhibit electrical activity in ICC

A and C, the effects of the GC activator YC-1 (30 μM) on STDs and STICS recorded under current clamp and voltage clamp, respectively. B and D, summary data of the effect of YC-1 on STD and STIC frequency obtained from five and six cells, respectively. E and G, the inhibitory effects of the membrane-permeant analogue of cGMP, 8-Br-cGMP (1 mM) on STDs and STICS recorded under current clamp and voltage clamp, respectively. F and H, summary data of the effect of 8-Br-cGMP on STDs and STICS obtained from four cells recorded under the same conditions as those in E and G, respectively.

DEA-NO reduced the amplitude of the waves ($\Delta F/F_0$) from 1.62 ± 0.34 to 0.58 ± 0.13 . The reason for the reduction in amplitude became apparent when the spatial spread of the Ca^{2+} waves was examined. Figure 3B shows a *post hoc* pseudo linescan (PLS) obtained by measuring the peak intensity of a 1 pixel-wide line drawn through the centre of the cell along its entire longitudinal axis

and plotting data against time. As shown in Fig. 3B the results suggest that under control conditions the Ca^{2+} waves spread $\sim 80 \mu\text{m}$. In the presence of $30 \mu\text{M}$ DEA-NO, spatial attenuation of the waves occurred. This effect was reversible upon washout. Figure 3C and D are profile plots through ROI 1, close to the site where the wave originated and ROI 2 which was $60 \mu\text{m}$ distal to the

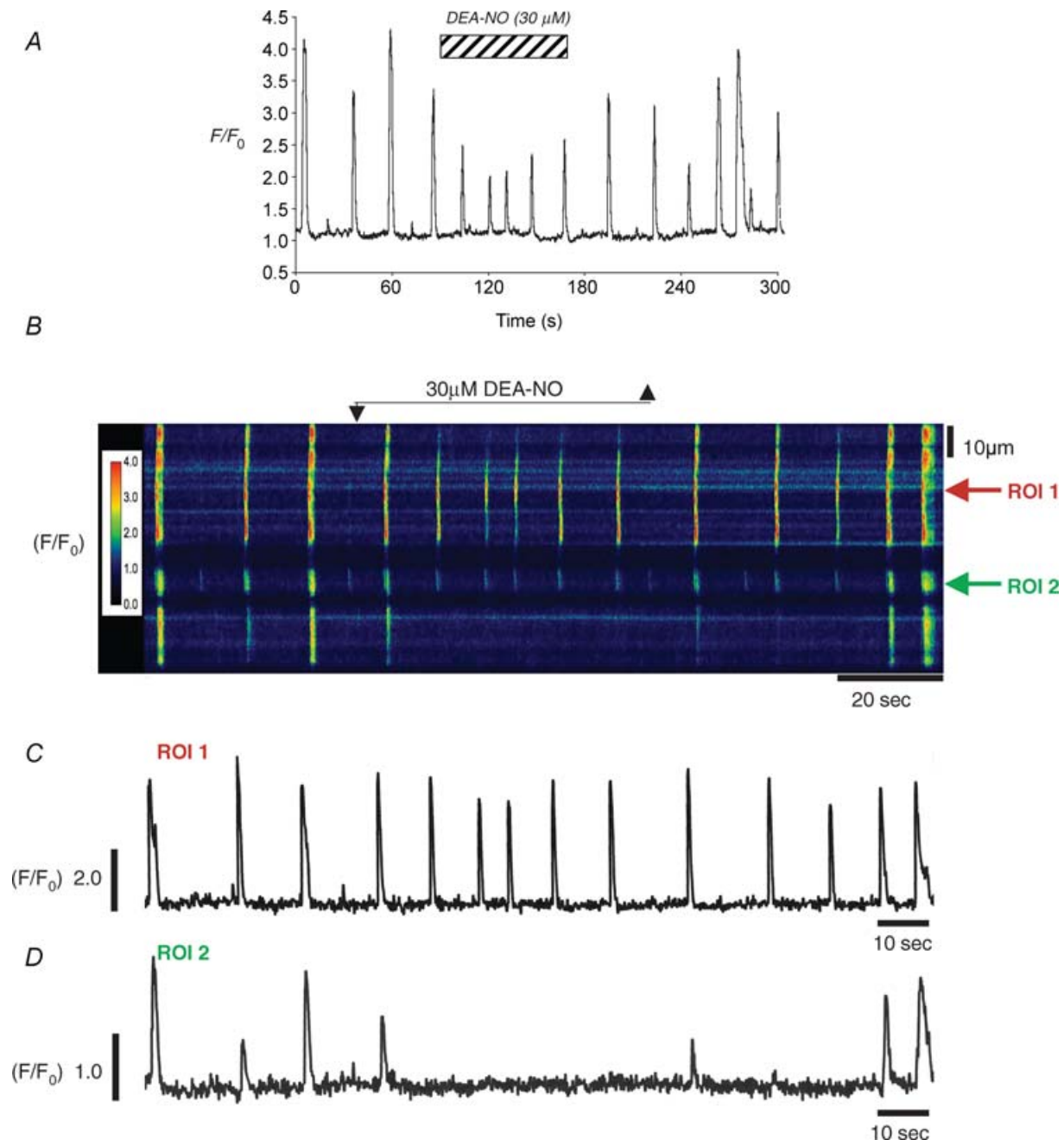


Figure 3. DEA-NO reduces whole-cell Ca^{2+} waves by reducing their spatial spread

A, a plot of whole-cell fluorescence before during and after application of DEA-NO. B, a pseudo-line scan of the same cell demonstrating that DEA-NO reversibly reduced wave spread. C, the oscillations at the site of origin were little affected by DEA-NO application, but they failed to spread to adjacent regions (D).

site of wave origin. Prior to drug application, two of the three control waves propagated without significant decrement from ROI 1 to ROI 2. However, in the presence of DEA-NO, although ROI 1 continued to fire (at a slightly increased frequency and reduced amplitude, in this example), none of these events were propagated to ROI 2. In six similar experiments summarized in Fig. 4, DEA-NO reversibly decreased the mean wave spread from $121 \pm 10 \mu\text{m}$ to $55 \pm 6 \mu\text{m}$ ($P < 0.01$), increased the basal fluorescence, and reduced the mean amplitude of the whole cell waves. However, the frequency of waves was unaffected by DEA-NO (5.9 ± 1.3 compared to $6.2 \pm 1.2 \text{ min}^{-1}$).

Effect of 8-Br-cGMP and YC-1 on spontaneous Ca^{2+} events

The reduction in spatial spread of the waves observed in the presence of DEA-NO was also apparent when either YC-1 or 8-Br-cGMP was applied. Figure 5A shows a typical example of the effects of activating a guanylyl cyclase (GC) with YC-1 ($30 \mu\text{M}$). Under control conditions the cell fired propagating waves, but upon application of YC-1 a reduction in the spatial spread of the Ca^{2+} wave was apparent without any significant reduction in wave frequency. Figure 5B shows profile plots of the fluorescence taken from two ROIs spaced $60 \mu\text{m}$ apart. In the absence of any drugs, the wave propagated without significant reduction in amplitude from ROI 1 to ROI 2. Although the waves still initiated close to ROI 1 in the presence of YC-1, they failed to propagate to ROI 2. Figure 5C and D shows summary data from seven experiments in which spatial spread was reduced from $89.7 \pm 9.2 \mu\text{m}$ to $27.8 \pm 5.5 \mu\text{m}$ ($P < 0.01$) by YC-1. However, frequency was little changed ($5.9 \pm 1.3 \text{ min}^{-1}$ under control conditions compared to $6.1 \pm 1.2 \text{ min}^{-1}$ in the presence of YC-1).

Figure 6A shows an example of spontaneous waves before and during application of 8-Br-cGMP (1 mM). Under control conditions, waves propagated throughout the cell (Fig. 6A). Application of 8-Br-cGMP increased basal fluorescence and reduced the spatial spread of the waves without affecting wave frequency. Summary data from six similar experiments is shown in Fig. 6B, where 8-Br-cGMP reduced the mean amplitude of the whole-cell waves, decreased the spatial spread of the waves from 98 ± 12 to $45 \pm 9 \mu\text{m}$, but again failed to significantly alter wave frequency ($3.9 \pm 0.7 \text{ min}^{-1}$ before compared to $4.9 \pm 0.7 \text{ min}^{-1}$ during cGMP). In approximately 30% of experiments 8-Br-cGMP evoked a transient release of Ca^{2+} upon application, followed by a transient inhibition of spontaneous activity. These data were excluded from the above analysis.

cGMP is thought to mediate its inhibitory effects via activation of PKG in the urethra. Therefore we tested if the PKG agonist, SP-8-Br-PET-cGMPs, produced similar

effects to those obtained with DEA-NO, 8-Br-cGMP and YC-1. Figure 7A shows the effect of $25 \mu\text{M}$ SP-8-Br-PET-cGMPs on spontaneous Ca^{2+} waves. In its presence, both the amplitude and spatial spread of waves were decreased, but again, frequency was little affected. In Fig. 7B, the mean fluorescence was measured and plotted against time at two ROIs placed $40 \mu\text{m}$ apart. In this example, the amplitude of the wave at the initiation site was also reduced. Figure 7C and D shows summary data for five experiments in which application of SP-8-Br-PET-cGMPs ($25 \mu\text{M}$) decreased spatial spread from $89 \pm 26 \mu\text{m}$ to $35 \pm 12 \mu\text{m}$ ($P < 0.01$), but had little effect on Ca^{2+} wave frequency ($5.3 \pm 0.5 \text{ min}^{-1}$ compared to $5.9 \pm 0.5 \text{ min}^{-1}$ $P = 0.21$).

Since release of Ca^{2+} from RyRs and IP_3 Rs plays an important role in the initiation and propagation of Ca^{2+} waves in urethral ICC (Johnston *et al.* 2005), we next tested if Ca^{2+} release from these stores was affected by

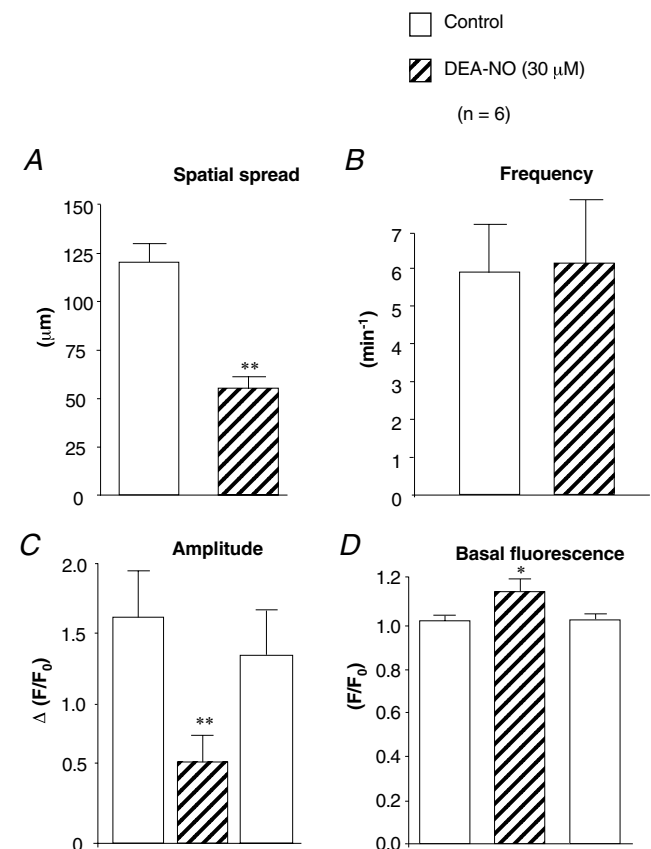


Figure 4. Summary data of the effect of DEA-NO

Summary bar charts showing the effect of DEA-NO ($30 \mu\text{M}$) on mean wave spread (μm) (A), mean frequency (min^{-1}) (B), mean whole cell wave amplitude ($\Delta F/F_0$) (C) and mean basal Ca^{2+} fluorescence (F/F_0) (D) in 6 cells. Experiments were performed under the same conditions as those shown in Fig. 3.

activation of the cGMP/PKG pathway. Noradrenaline (NA, 10 μM) and caffeine (1 mM) were used to induce Ca^{2+} release via IP_3Rs and RyRs, respectively, in cells held under voltage clamp at -60 mV. Under control conditions, NA application for 10 s induced a transient Ca^{2+} -activated Cl^- current, due to release of Ca^{2+} via IP_3Rs (Sergeant *et al.* 2002). As Fig. 8A suggests, activation of PKG with SP-8-Br-PET-cGMPs (25 μM) reversibly reduced the amplitude of these currents. Summary data from six similar experiments shown in Fig. 8B demonstrate that PKG activation decreased NA-evoked Cl^- currents from -750 ± 198 pA to -333 ± 98 pA ($P < 0.01$). In contrast, as Fig. 8C demonstrates, SP-8-Br-PET-cGMPs (25 μM) had little effect on Ca^{2+} release via RyRs evoked by 1 mM caffeine (Sergeant, 2000). The bar chart in Fig. 8D shows summary data from five similar experiments. The mean amplitude of the caffeine-evoked currents was -614 ± 203 pA under control conditions compared to -557 ± 169 pA in SP-8-Br-PET-cGMPs ($P = 0.2$). Ca^{2+} release evoked by 1 mM caffeine was unaffected in the

presence of 2-APB (100 μM , $n = 4$), suggesting that this concentration of caffeine did not cause release of Ca^{2+} from IP_3Rs . In four separate experiments, we also examined the effects of SP-8-Br-PET-cGMPs (25 μM) on Cl^- currents evoked by 10 mM caffeine in cells held at -60 mV. Under control conditions the peak current evoked by 10 mM caffeine was -1027 ± 256 pA, compared to -1049 ± 371 pA in the presence of SP-8-Br-PET-cGMPs. These data suggest that activation of PKG inhibits release of Ca^{2+} from IP_3Rs but not RyRs. Furthermore, the inability of SP-8-Br-PET-cGMPs to inhibit Cl^- currents activated by caffeine suggests that the PKG activator does not directly inhibit Cl^- channels.

The data above support the idea that activators of PKG modulate Ca^{2+} release via IP_3Rs . We therefore tested the effect of inhibiting IP_3Rs with 2-APB on spontaneous Ca^{2+} waves, to examine if it mimicked the effect of activating the cGMP/PKG pathway. Figure 9A shows a typical example of one such experiment in which Ca^{2+} waves were recorded at 15 fps. After the cell had fired

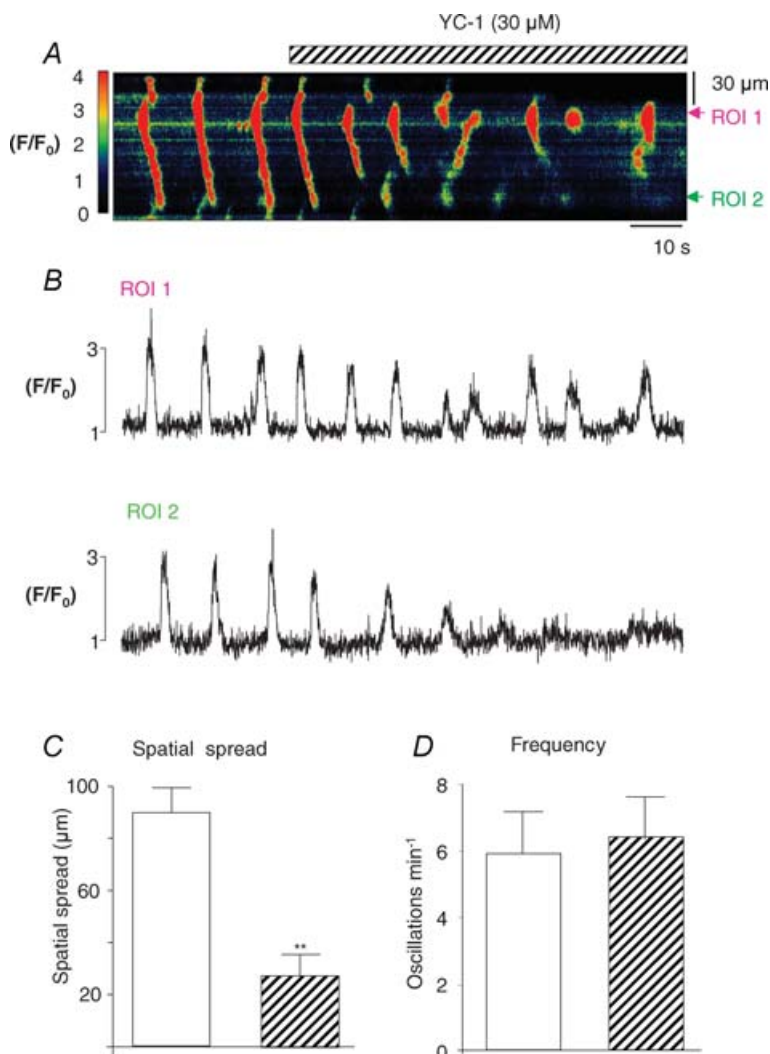


Figure 5. The effect of activating GC on Ca^{2+} waves

A, a line scan image of global Ca^{2+} waves in the absence and presence of YC-1 (30 μM). B, two profile plots taken from ROI 1 and ROI 2. C, summary graphs of the effects of YC-1 on mean Ca^{2+} spread (μm) and D, mean frequency (min^{-1}).

four waves, 2-APB ($100 \mu\text{M}$) was applied. Although the cell still produced oscillations, their spatial spread was markedly attenuated. The frequency of waves was reduced in this experiment, but in 11 similar experiments it was not significantly altered (from $4.8 \pm 0.5 \text{ min}^{-1}$ under control conditions compared to $4.1 \pm 0.4 \text{ min}^{-1}$ in 2-APB, $P = 0.14$, Fig. 9D). However, in the same 11 experiments, application of 2-APB significantly reduced the spatial spread of the Ca^{2+} waves from $115 \pm 11 \mu\text{m}$ to $44 \pm 5 \mu\text{m}$ ($P < 0.01$, Fig. 9C). In a separate series of experiments, we also examined the effects of inhibiting phospholipase C with $100 \mu\text{M}$ NCDC. In six cells, NCDC application significantly decreased the spatial spread of the Ca^{2+} waves from $121 \pm 19 \mu\text{m}$ to $45 \pm 9 \mu\text{m}$ ($P < 0.01$) without affecting wave frequency or basal Ca^{2+} . The above data are consistent with the idea that activation of the cGMP/PKG pathway inhibits Ca^{2+} release via IP_3Rs .

Figure 10 shows recordings from an ICC in which we simultaneously recorded membrane potential and

Ca^{2+} waves before and during SP-8-Br-PET-cGMPs application. Hyperpolarizing background current was injected to bring membrane potential to $\sim -70 \text{ mV}$. The red vertical lines in Fig. 10A are artifacts caused by the regular emission of an LED used to synchronize the fluorescence capture and electrophysiological recordings. Figure 10B shows a plot of whole-cell fluorescence (in red) and membrane potential (in black) from the same experiment. Prior to PKG activation, the cell produced large phasic increases in Ca^{2+} , which triggered full STDs. Occasionally smaller Ca^{2+} release events were detected. These produced small-amplitude transient fluctuations in membrane potential that depolarized the cell by $< 25 \text{ mV}$, but failed to reach threshold (-40 mV) to activate the L-type Ca^{2+} channels and elicit full STDs. In the presence of SP-8-Br-PET-cGMPs, the Ca^{2+} waves were clearly attenuated, and small-amplitude Ca^{2+} release events that spread $< 20 \mu\text{m}$ were apparent. In this experiment, one Ca^{2+} event was sufficiently large to depolarize the cell to

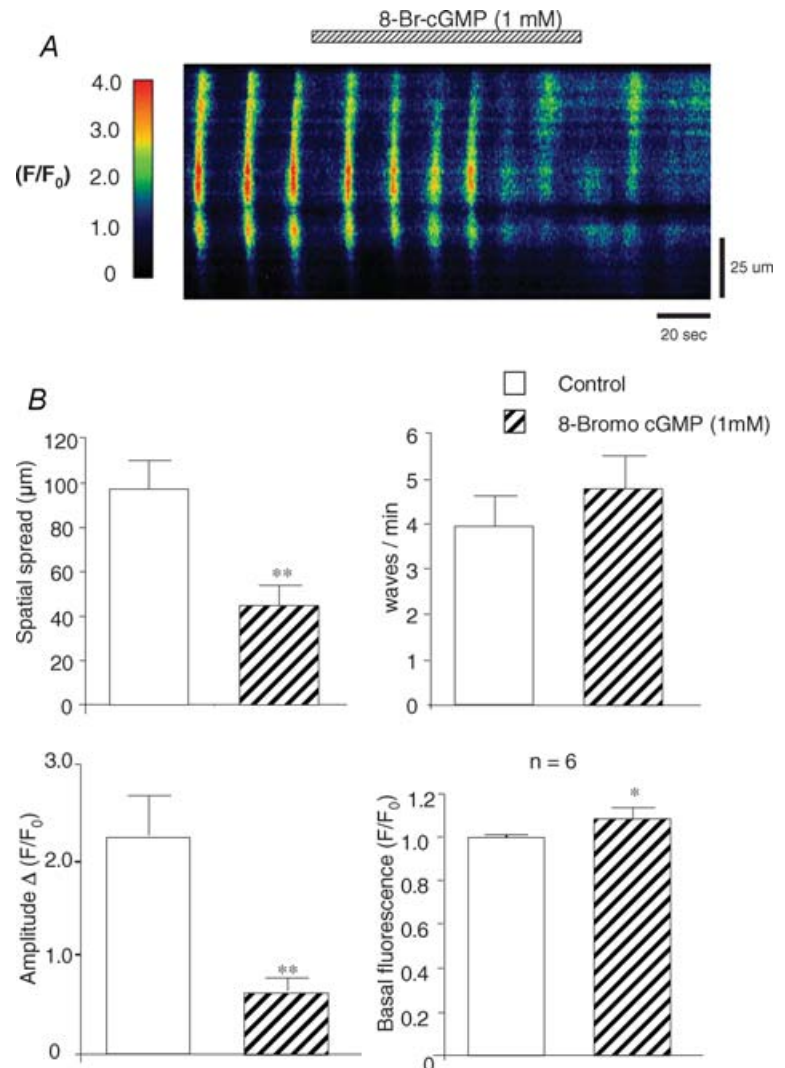


Figure 6. The effect of 8-Br-cGMP on Ca^{2+} waves

A line scan image showing global Ca^{2+} waves in the absence and presence of 8-Br-cGMP (1 mM). B, summary graphs showing the effects of cGMP on mean Ca^{2+} spread (μm), mean frequency (min^{-1}), mean amplitude ($\Delta F/F_0$) and basal Ca^{2+} fluorescence (F/F_0) $n = 6$.

~ -40 mV, and elicited a large STD after approximately 60 s exposure to SP-8-Br-PET-cGMPs. Upon washout of SP-8-Br-PET-cGMPs, wave amplitude and STD frequency returned towards control values.

Discussion

Although the cGMP/GK₁ pathway contributes to NO-mediated relaxations in the urethra, little is known about the cellular targets for cGMP/GK₁, or how NO affects electrical activity in the urethra. In vascular smooth muscle, NO is thought to activate K⁺ channels either directly (Bolotina *et al.* 1994) or indirectly via stimulation of the cGMP/PKG pathway (Carrier *et al.* 1997). Consequently, membrane hyperpolarization occurs, Ca²⁺ influx is reduced, and relaxation occurs (Carrier *et al.* 1997; Heppner *et al.* 2003). In the urethra however, the neurogenic relaxation appears to be resistant to K⁺ channel

blockade (Costa *et al.* 2001), suggesting that these channels contribute little to NO-induced relaxation. Intracellular recordings by Waldeck *et al.* (1998) and Hashitani *et al.* (1996) have similarly failed to demonstrate any change in membrane potential induced by either NO donors or cGMP analogues in rabbit urethral circular muscle, suggesting that NO does not act by hyperpolarizing the tissue. However, the latter study demonstrated that sodium nitroprusside and 8-Br-cGMP reduced the frequency of STDs recorded from rabbit urethral circular smooth muscle.

Since this spontaneous activity is thought to arise from ICC in the urethra (Sergeant *et al.* 2000) it is conceivable that neurotransmitters may mediate their effects on tone by modulating activity in these cells. Burns *et al.* (1996) and Beckett *et al.* (2002) have provided compelling evidence to suggest that ICC play an important role in neurotransmission in the gastrointestinal tract, since knockout

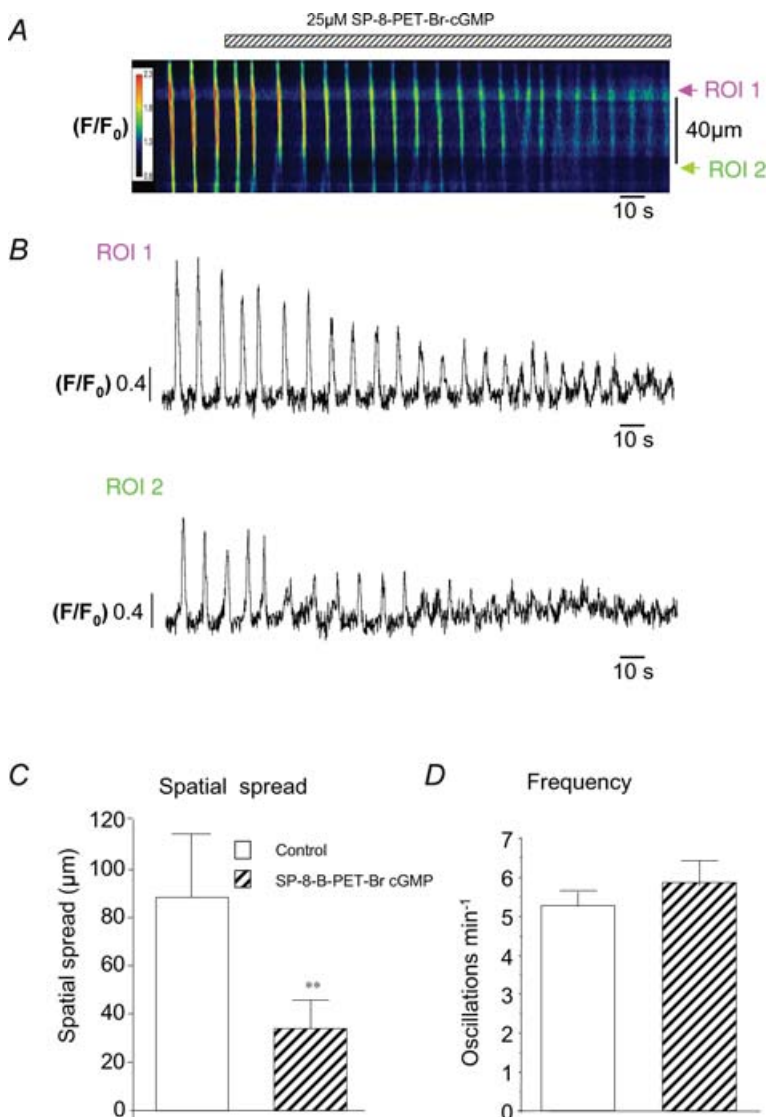


Figure 7. The effect of the G-kinase activator SP-8-Br-PET-cGMP on Ca²⁺ waves

A, a pseudo-line scan image of propagated Ca²⁺ waves in the absence and presence of the G-kinase activator SP-8-Br-PET-cGMPs (25 μM). B, profile plots taken from the two specific regions in the cell (labelled ROI 1 and ROI 2 in A placed 30 μm apart). C and D, summary data to demonstrate that G-kinase activation significantly reduced wave spatial spread but had no significant effect on wave frequency, respectively.

mice lacking ICC have severely attenuated neurogenic responses. A number of studies suggest that ICC may also contribute to neurotransmission in the urethra. Previous results from our laboratory demonstrate that urethral ICC respond to exogenous NA application, and when these ICC are pharmacologically ablated, the contractile responses to adrenergic neurotransmission are abolished (Sergeant *et al.* 2002). Smet *et al.* (1996) have provided immunohistochemical evidence in the guinea-pig and human urethra, that cells with a morphological appearance similar to ICC in the gut, may also play a role in inhibitory neurotransmission. Their demonstration that ICC were immunopositive for cGMP following incubation of the tissues with NO donors, suggests that these cells possess the biochemical pathways to respond to NO.

The results of the present study are consistent with the findings of Smet *et al.* (1996) and demonstrate that spontaneous electrical activity in ICC is inhibited by activators of the cGMP/PKG pathway. Thus, DEA-NO, YC-1 and 8-Br-cGMP reversibly decreased the frequency of STDs in cells studied under current clamp. Similarly, under voltage-clamp conditions, the amplitude and frequency of STICs were also reduced by activators of the cGMP/PKG

pathway. A number of possibilities could account for these inhibitory effects on electrical activity: (1) Ca^{2+} influx was reduced; (2) Cl^- channels were directly inhibited; or (3) Ca^{2+} mobilization from intracellular stores was altered. Although a number of studies have demonstrated that NO can inhibit Ca^{2+} influx through either voltage-gated Ca^{2+} channels (Blatter & Wier, 1994; Grassi *et al.* 2004) or capacitative Ca^{2+} entry (CCE) pathways (Trepakova *et al.* 1999), this is unlikely to account for our observations for a number of reasons. Firstly, inhibition of L-type Ca^{2+} channels in urethral ICC has no effect on the frequency of either STDs or STICs (Sergeant *et al.* 2000). Although complete inhibition of T-type Ca^{2+} channels with $100 \mu\text{M}$ Ni^{2+} has been demonstrated to decrease the frequency of STICs in urethral ICC (Bradley *et al.* 2005), the effects were rather modest ($\sim 25\%$ reduction). It is equally unlikely that inhibition of CCE is responsible, since blockade of CCE with either Gd^{3+} or La^{3+} failed to significantly alter STIC frequency in urethral ICC (Bradley *et al.* 2005).

The ability of caffeine to evoke robust Cl^- currents in the presence of SP-8-Br-PET-cGMPs suggests that PKG activation did not directly block the Cl^- currents in these cells. Furthermore, since caffeine is thought to

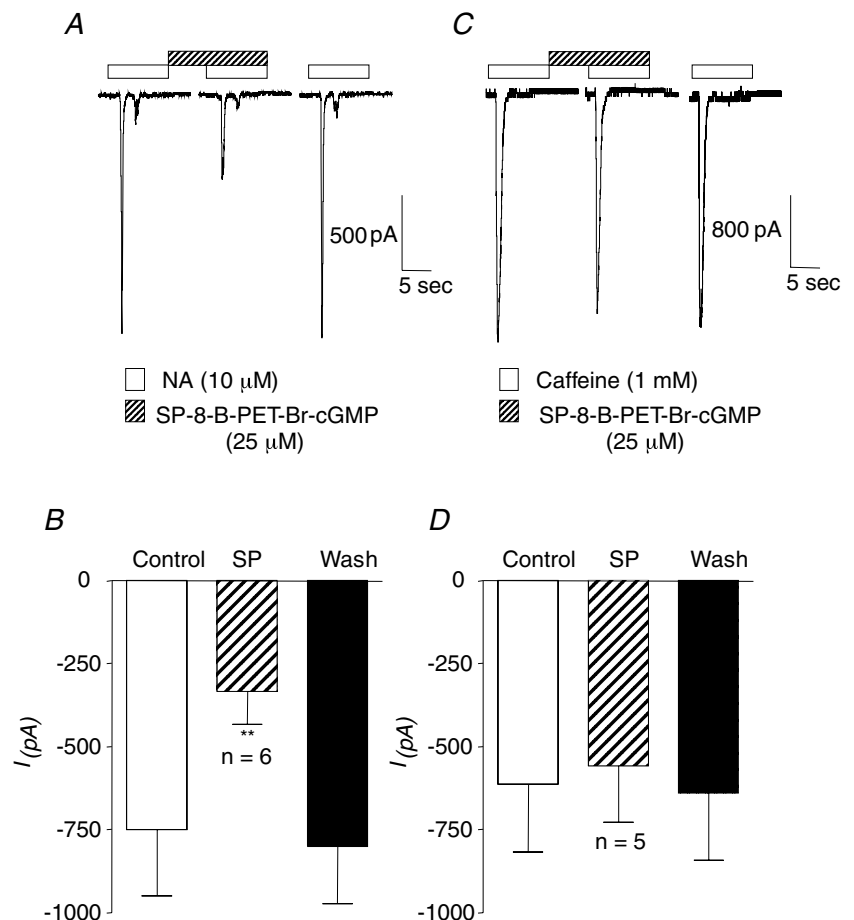


Figure 8. Activating PKG inhibits Ca^{2+} release from IP_3Rs but not RyRs

A shows NA-evoked currents recorded under voltage clamp at -60 mV , before, during and after activation of PKG with SP-8-Br-PET-cGMPs; 80 s intervals were left between successive intervals of NA. B, summary data for the effect of SP-8-Br-PET-cGMPs on NA-evoked currents. C, caffeine-evoked currents before, during and after activation of PKG with SP-8-Br-PET-cGMPs. Caffeine was applied at 80 s intervals. D, summary data for the effect of SP-8-Br-PET-cGMPs on caffeine-evoked currents.

enhance release of Ca^{2+} from the sarcoplasmic reticulum (SR) via RyR activation (Zucchi & Ronca-Testoni, 1997), it appears that Ca^{2+} release through these channels remained intact in the presence of the PKG agonist. In contrast, when Ca^{2+} release via IP_3Rs was triggered with exogenous noradrenaline (Sergeant *et al.* 2002), the amplitude of the evoked current was significantly reduced by SP-8-Br-PET-cGMPs. These data suggest that activation of PKG may specifically interfere with release of Ca^{2+} from IP_3R receptors, as has been suggested in rabbit corpus cavernosal and guinea-pig ileal myocytes (Craven *et al.* 2004; Chung *et al.* 2005).

To further examine how activation of the NO/cGMP pathway altered Ca^{2+} mobilization from intracellular stores, we carried out experiments on ICC loaded with Fluo4-AM. We found that the ICC displayed a variety of Ca^{2+} events, the most common consisting of spontaneous propagating Ca^{2+} waves as noted previously (Johnston *et al.* 2005). We previously demonstrated that these spontaneous waves were abolished by either ryanodine or

tetracaine, suggesting that RyR activation was critical for the initiation of Ca^{2+} waves in ICC (Johnston *et al.* 2005). In contrast, the IP_3R blocker 2-APB (Maruyama *et al.* 1997), reduced the amplitude of Ca^{2+} waves, indicating that the IP_3Rs serve to amplify the initial Ca^{2+} signal and permit the propagation of waves (Johnston *et al.* 2005). 2-APB has been shown to be unselective in a number of studies, and has been demonstrated to block Ca^{2+} influx, and inhibit Ca^{2+} uptake in addition to its inhibitory effects on Ca^{2+} release on IP_3R (Peppiat *et al.* 2003). However, we have found little evidence to suggest that it produces these effects in rabbit urethral ICC. Thus, it selectively blocks STICS but not STOCs in these cells, suggesting that it does not block Ca^{2+} release from RyRs but does inhibit release via IP_3Rs (Sergeant *et al.* 2001). Similarly, it does not block caffeine-evoked Cl^- currents, but does block IP_3R -mediated Ca^{2+} release induced by noradrenaline (Sergeant *et al.* 2002). We have demonstrated that 2-APB can modestly block capacitative Ca^{2+} entry (20%) in urethral ICC (Bradley *et al.* 2005); other more

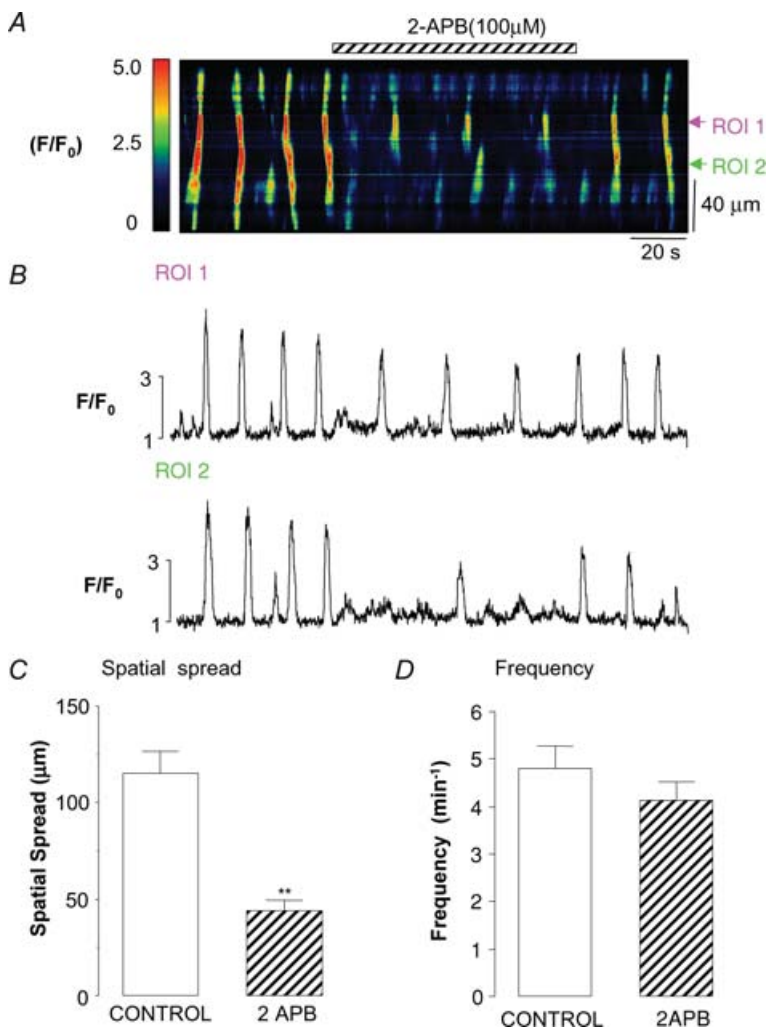


Figure 9. Inhibition of Ca^{2+} release via IP_3Rs mimics the effect of NO on Ca^{2+} waves

A, pseudo-line scan image of propagated Ca^{2+} waves in the absence and presence of the IP_3R inhibitor 2-APB (100 μM). *B*, two profile plots taken from two ROIs placed 40 μm apart. *C* and *D*, summaries of the effect of 2-APB on spatial spread and wave frequency.

potent blockers of CCE have little effect on spontaneous activity suggesting that CCE plays little role in modulating the spontaneous activity observed.

Although application of DEA-NO failed to reduce the frequency of the Ca^{2+} oscillations, it dramatically reduced whole-cell wave amplitude. These effects were mimicked by both 8-Br-cGMP and SP-8-Br-PET-cGMPs, supporting the idea that NO mediates its effects via cGMP and GK_1 as suggested by Persson *et al.* (2000). The reduction in whole-cell wave amplitude was largely explained by a significant decrease in the spatial spread of waves. In some examples the wave amplitude at the initiation site was also reduced (see Fig. 7A). Although this latter effect could contribute to the reduction in the spatial spread of the waves, the fact that spatial attenuation was often observed without any significant reduction in the amplitude of the wave at the initiation site (see Fig. 3B & C), suggests that the cGMP/PKG pathway can inhibit wave propagation independently of an effect on the primary pacemaker Ca^{2+} -release site. However, given that RyRs appear not to be modulated by cGMP/PKG in our cells, the above data also suggest that a subpopulation of primary pacemaker Ca^{2+} release sites consist of clusters of both RyRs and IP_3 Rs as has been suggested in hippocampal neurons (Koizumi *et al.* 1999), arterial smooth muscle (Boittin *et al.* 1998) and cardiac myocytes (Lipp *et al.* 2000).

Activation of the NO/cGMP pathway produced effects on Ca^{2+} waves that were similar to those of IP_3 R blockade

with 2-APB or inhibition of phospholipase C (PLC) with NCDC. These data are consistent with the idea that NO may mediate its effects on urethral ICC by modulating Ca^{2+} release from IP_3 Rs or by inhibiting IP_3 production. A number of studies have demonstrated that PKG can either reduce IP_3 production (Murthy *et al.* 1993; Ruth *et al.* 1993; Ding & Abdel-Latif, 1997) or inhibit Ca^{2+} release from IP_3 Rs (Komalavilas & Lincoln, 1996; Tertyschnikova *et al.* 1998; Feil *et al.* 2002; Murthy & Zhou, 2003). The mechanism through which PKG inhibits Ca^{2+} release via IP_3 Rs is a matter of debate and varies between tissues. Murthy & Zhou (2003) suggested that $\text{PKG}_{1\alpha}$ directly phosphorylated IP_3 Rs in gastric smooth muscle cells to inhibit Ca^{2+} release. However, Schlossmann *et al.* (2000) have argued that $\text{PKG}_{1\beta}$ first phosphorylates a novel protein – inositol 1,4,5-trisphosphate receptor-associated cGMP kinase substrate (IRAG), which in turn modulates the IP_3 R to reduce Ca^{2+} release. In support of this, Fritsch *et al.* (2004) found that NO/PKG-dependent inhibition of Ca^{2+} signalling in human colonic myocytes was abolished in cells treated with antisense oligonucleotides raised against IRAG, suggesting that IRAG was essential for mediating the effects of NO in these myocytes. Whether a similar mechanism is responsible for the inhibitory effects of NO in the urethra remains to be determined.

Regardless of how activation of the cGMP/PKG pathway inhibits Ca^{2+} release via IP_3 Rs, it is tempting to speculate on how decreased Ca^{2+} wave amplitude leads to a

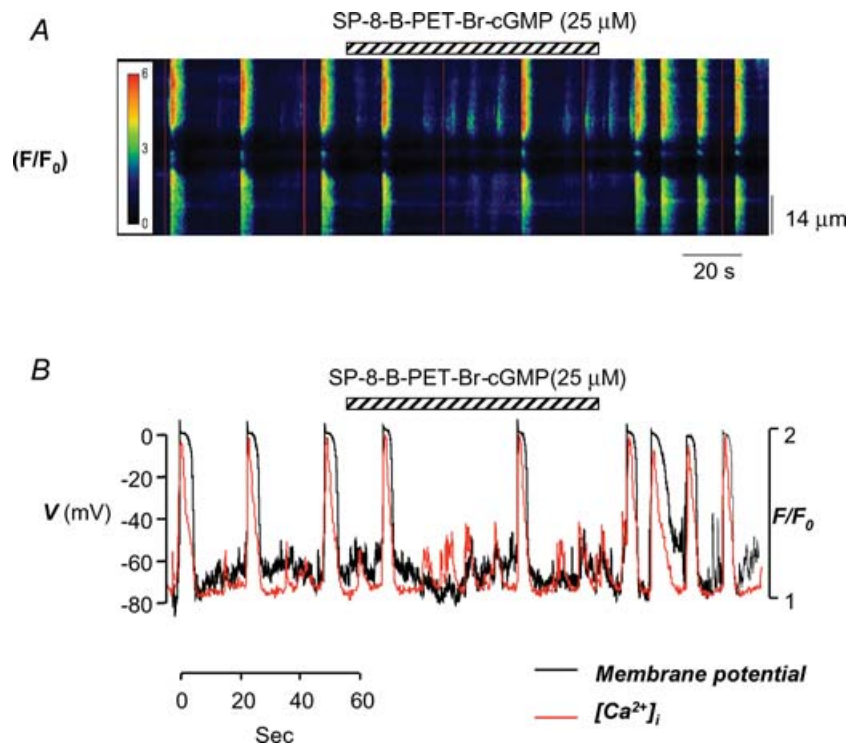


Figure 10. PKG activation reduces STD frequency by inhibiting wave spread

A, pseudo-line scan image of a spontaneously active ICC loaded with Fluo4-AM and held under current-clamp conditions. Application of SP-8-Br-PET-cGMPs ($25 \mu\text{M}$) reduced the frequency of Ca^{2+} oscillations and unmasked smaller Ca^{2+} release events. B, a plot of whole-cell fluorescence (red) and membrane potential (black) before during and after application SP-8Br-PET-cGMPs.

decrease in STD frequency. We hypothesize that a reduction in the spatial spread of the Ca^{2+} signal in urethral ICCs would effectively limit the coupling between $[\text{Ca}^{2+}]_i$ and the Cl^- channels. As a consequence of this functional uncoupling, each Ca^{2+} oscillation fails to activate sufficient Cl^- channels to depolarize the ICC and bring it into the range to fire STDs. This prevents activation of voltage-dependent Ca^{2+} channels, and limits the propagation of the pacemaking signal to the smooth muscle. In the absence of such a pacemaking 'drive', the ICC fail to rhythmically depolarize the smooth muscle and thus, the smooth muscle fails to fire action potentials. This decrease in action potential firing frequency in the smooth muscle leads to a reduction in smooth muscle cell $[\text{Ca}^{2+}]_i$, and ultimately reduces urethral tone.

References

- Andersson KE & Wein AJ (2004). Pharmacology of the lower urinary tract: basis for current and future treatments of urinary incontinence. *Pharmacol Rev* **56**, 581–631.
- Beckett EA, Horiguchi K, Khoyi M, Sanders KM & Ward SM (2002). Loss of enteric motor neurotransmission in the gastric fundus of SI/SI(d) mice. *J Physiol* **543**, 871–887.
- Blatter LA & Wier WG (1994). Nitric oxide decreases $[\text{Ca}^{2+}]_i$ in vascular smooth muscle by inhibition of the calcium current. *Cell Calcium* **15**, 122–131.
- Boittin FX, Coussin F, Macrez N, Mironneau C & Mironneau J (1998). Inositol 1,4,5-trisphosphate- and ryanodine-sensitive Ca^{2+} release channel-dependent Ca^{2+} signalling in rat portal vein myocytes. *Cell Calcium* **23**, 303–311.
- Bolotina VM, Najibi S, Palacino JJ, Pagano PJ & Cohen RA (1994). Nitric oxide directly activates calcium-dependent potassium channels in vascular smooth muscle. *Nature* **368**, 850–853.
- Bradley E, Hollywood MA, McHale NG, Thornbury KD & Sergeant GP (2005). Pacemaker activity in urethral interstitial cells is not dependent on capacitative calcium entry. *Am J Physiol Cell Physiol* **289**, C625–C632.
- Burns AJ, Lomax AE, Torihashi S, Sanders KM & Ward SM (1996). Interstitial cells of Cajal mediate inhibitory neurotransmission in the stomach. *Proc Natl Acad Sci U S A* **93**, 12008–12013.
- Carrier GO, Fuchs LC, Winecoff AP, Giuliumian AD & White RE (1997). Nitrovasodilators relax mesenteric microvessels by cGMP-induced stimulation of Ca-activated K channels. *Am J Physiol* **273**, H76–H84.
- Chung SS, Ahn DS, Lee HG, Lee YH & Nam TS (2005). Inhibition of carbachol-evoked oscillatory currents by the NO donor sodium nitroprusside in guinea-pig ileal myocytes. *Exp Physiol* **90**, 577–586.
- Costa G, Labadia A, Triguero D, Jimenez E & Garcia-Pascual A (2001). Nitrergic relaxation in urethral smooth muscle: involvement of potassium channels and alternative redox forms of no. *Naunyn Schmiedebergs Arch Pharmacol* **364**, 516–523.
- Craven M, Sergeant GP, Hollywood MA, McHale NG & Thornbury KD (2004). Modulation of spontaneous Ca^{2+} -activated Cl^- currents in the rabbit corpus cavernosum by the nitric oxide-cGMP pathway. *J Physiol* **556**, 495–506.
- Ding KH & Abdel-Latif AA (1997). Actions of C-type natriuretic peptide and sodium nitroprusside on carbachol-stimulated inositol phosphate formation and contraction in ciliary and iris sphincter smooth muscles. *Invest Ophthalmol Vis Sci* **38**, 2629–2638.
- Dokita S, Smith SD, Nishimoto T, Wheeler MA & Weiss RM (1994). Involvement of nitric oxide and cyclic GMP in rabbit urethral relaxation. *Eur J Pharmacol* **266**, 269–275.
- Feil R, Gappa N, Rutz M, Schlossmann J, Rose CR, Konnerth A, Brummer S, Kuhbandner S & Hofmann F (2002). Functional reconstitution of vascular smooth muscle cells with cGMP-dependent protein kinase I isoforms. *Circ Res* **90**, 1080–1086.
- Fritsch RM, Saur D, Kurjak M, Oesterle D, Schlossmann J, Geiselhoring A, Hofmann F & Allescher HD (2004). InsP_3 -associated cGMP kinase substrate (IRAG) is essential for nitric oxide-induced inhibition of calcium signalling in human colonic smooth muscle. *J Biol Chem* **279**, 12551–12559.
- Garcia-Pascual A & Triguero D (1994). Relaxation mechanisms induced by stimulation of nerves and by nitric oxide in sheep urethral muscle. *J Physiol* **476**, 333–347.
- Grassi C, D'Ascenzo M & Azzena GB (2004). Modulation of $\text{Ca}(\nu)$, 1 and $\text{Ca}(\nu)$, 2.2 channels induced by nitric oxide via cGMP-dependent protein kinase. *Neurochem Int* **45**, 885–893.
- Hashitani H, Van Helden DF & Suzuki H (1996). Properties of spontaneous depolarizations in circular smooth muscle cells of rabbit urethra. *Br J Pharmacol* **118**, 1627–1632.
- Heppner TJ, Herrera GM, Bonev AD, Hill-Eubanks D & Nelson MT (2003). Ca^{2+} sparks and $\text{K}(\text{Ca})$ channels: novel mechanisms to relax urinary bladder smooth muscle. *Adv Exp Med Biol* **539**, 347–357.
- Ito Y & Kimoto Y (1985). The neural and non-neural mechanisms involved in urethral activity in rabbits. *J Physiol* **367**, 57–72.
- Johnston L, Sergeant GP, Hollywood MA, Thornbury KD & McHale NG (2005). Calcium oscillations in interstitial cells of the rabbit urethra. *J Physiol* **565**, 449–461.
- Koizumi S, Bootman MD, Bobanovic LK, Schell MJ, Berridge MJ & Lipp P (1999). Characterization of elementary Ca^{2+} release signals in NGF-differentiated PC12 cells and hippocampal neurons. *Neuron* **22**, 125–137.
- Komalavilas P & Lincoln TM (1996). Phosphorylation of the inositol 1,4,5-trisphosphate receptor. Cyclic GMP-dependent protein kinase mediates cAMP and cGMP dependent phosphorylation in the intact rat aorta. *J Biol Chem* **271**, 21933–21938.
- Lipp P, Laine M, Tovey SC, Burrell KM, Berridge MJ, Li W & Bootman MD (2000). Functional InsP_3 receptors that may modulate excitation-contraction coupling in the heart. *Curr Biol* **10**, 939–942.
- Maruyama T, Kanaji T, Nakade S, Kanno T & Mikoshiba K (1997). 2APB, 2-Aminoethoxydiphenyl borate, a membrane-penetrable modulator of $\text{Ins}(1,4,5)\text{P}_3$ -induced Ca^{2+} release. *J Biochem* **122**, 498–505.

- Morita T, Tsujii T & Dokita S (1992). Regional difference in functional roles of cAMP and cGMP in lower urinary tract smooth muscle contractility. *Urol Int* **49**, 191–195.
- Murthy KS, Severi C, Grider JR & Makhoulf GM (1993). Inhibition of IP₃ and IP₃-dependent Ca²⁺ mobilization by cyclic nucleotides in isolated gastric muscle cells. *Am J Physiol* **264**, G967–G974.
- Murthy KS & Zhou H (2003). Selective phosphorylation of the IP₃R-I in vivo by cGMP-dependent protein kinase in smooth muscle. *Am J Physiol Gastrointest Liver Physiol* **284**, G221–G230.
- Peppiatt CM, Collins TJ, Mackenzie L, Conway SJ, Holmes AB, Bootman MD, Berridge MJ, Seo JT & Roderick HL (2003). 2-Aminoethoxydiphenyl borate (2-APB) antagonises inositol 1,4,5-trisphosphate-induced calcium release, inhibits calcium pumps and has a use-dependent and slowly reversible action on store-operated calcium entry channels. *Cell Calcium* **34**, 97–108.
- Persson K & Andersson KE (1994). Non-adrenergic, non-cholinergic relaxation and levels of cyclic nucleotides in rabbit lower urinary tract. *Eur J Pharmacol* **268**, 159–167.
- Persson K, Pandita RK, Aszodi A, Ahmad M, Pfeifer A, Fassler R & Andersson KE (2000). Functional characteristics of urinary tract smooth muscles in mice lacking cGMP protein kinase type I. *Am J Physiol Regul Integr Comp Physiol* **279**, R1112–R1120.
- Rae J, Cooper K, Gates P & Watsky M (1991). Low access resistance perforated patch recordings using amphotericin B. *J Neurosci Meth* **37**, 15–26.
- Ruth P, Wang GX, Boekhoff I, May B, Pfeifer A, Penner R, Korth M, Breer H & Hofmann F (1993). Transfected cGMP-dependent protein kinase suppresses calcium transients by inhibition of inositol 1,4,5-trisphosphate production. *Proc Natl Acad Sci U S A* **90**, 2623–2627.
- Sanders KM, Koh SD & Ward SM (2005). Interstitial Cells of Cajal as Pacemakers in the Gastrointestinal Tract. *Annu Rev Physiol* October 24; **68**, 307–343.
- Schlossmann J, Ammendola A, Ashman K, Zong X, Huber A, Neubauer G, Wang GX, Allescher HD, Korth M, Wilm M, Hofmann F & Ruth P (2000). Regulation of intracellular calcium by a signalling complex of IRAG, IP₃ receptor and cGMP kinase Iβ. *Nature* **404**, 197–201.
- Sergeant GP (2000). *Specialised Pacemaking Cells in the Rabbit Urethra*. PhD Thesis, The Queens University of Belfast.
- Sergeant GP, Hollywood MA, McCloskey KD, Thornbury KD & McHale NG (2000). Specialised pacemaking cells in the rabbit urethra. *J Physiol* **526**, 359–366.
- Sergeant GP, Thornbury KD, McHale NG & Hollywood MA (2002). Characterization of norepinephrine-evoked inward currents in interstitial cells isolated from the rabbit urethra. *Am J Physiol Cell Physiol* **283**, C885–C894.
- Smet PJ, Jonavicius J, Marshall VR & De Vente J (1996). Distribution of nitric oxide synthase-immunoreactive nerves and identification of the cellular targets of nitric oxide in guinea-pig and human urinary bladder by cGMP immunohistochemistry. *Neuroscience* **71**, 337–348.
- Tertyshnikova S, Yan X & Fein A (1998). cGMP inhibits IP₃-induced Ca²⁺ release in intact rat megakaryocytes via cGMP- and cAMP-dependent protein kinases. *J Physiol* **512**, 89–96.
- Trepakova ES, Cohen RA & Bolotina VM (1999). Nitric oxide inhibits capacitative cation influx in human platelets by promoting sarcoplasmic/endoplasmic reticulum Ca²⁺-ATPase-dependent refilling of Ca²⁺ stores. *Circ Res* **84**, 201–209.
- Waldeck K, Ny L, Persson K & Andersson KE (1998). Mediators and mechanisms of relaxation in rabbit urethral smooth muscle. *Br J Pharmacol* **123**, 617–624.
- Zucchi R & Ronca-Testoni S (1997). The sarcoplasmic reticulum Ca²⁺ channel/ryanodine receptor: modulation by endogenous effectors, drugs and disease states. *Pharmacol Rev* **49**, 1–51.

Acknowledgements

The authors acknowledge the financial support of NIDDK (Grant R01-DK68565) and the Wellcome Trust (Grant: 064212). Louise Johnston was in receipt of a DEL (NI) Post Graduate Studentship and Gerard Sergeant is in receipt of a Health Research Board Post-Doctoral Fellowship. The authors would like to thank Dr Tony Collins, Wright Cell Imaging Facility, Toronto, Canada, for writing the Image J macros used in the data analysis.

Author's present address

L. Johnston: Queens University of Belfast, 97 Lisburn Road, Belfast BT9 7BL, Northern Ireland, UK.